PLUMES – REACTIVE DIFFUSION

1. EVOLUTION OF PLUMES

1.1 NATURAL ATTENUATION

As discussed in former chapters source zones may last for very long time periods especially if NAPL sources are concerned. Therefore, plumes have plenty of time to develop and theoretically may continue to grow especially if retardation of the contaminant is low (e.g., well soluble compounds such as chlorinated solvents or PFAS). However, plumes of biodegradable compounds (e.g., BTEX) may remain quite short, if the emission rate from the source is balanced by the overall degradation rate as shown in Figs. 1.1 and 1.2.

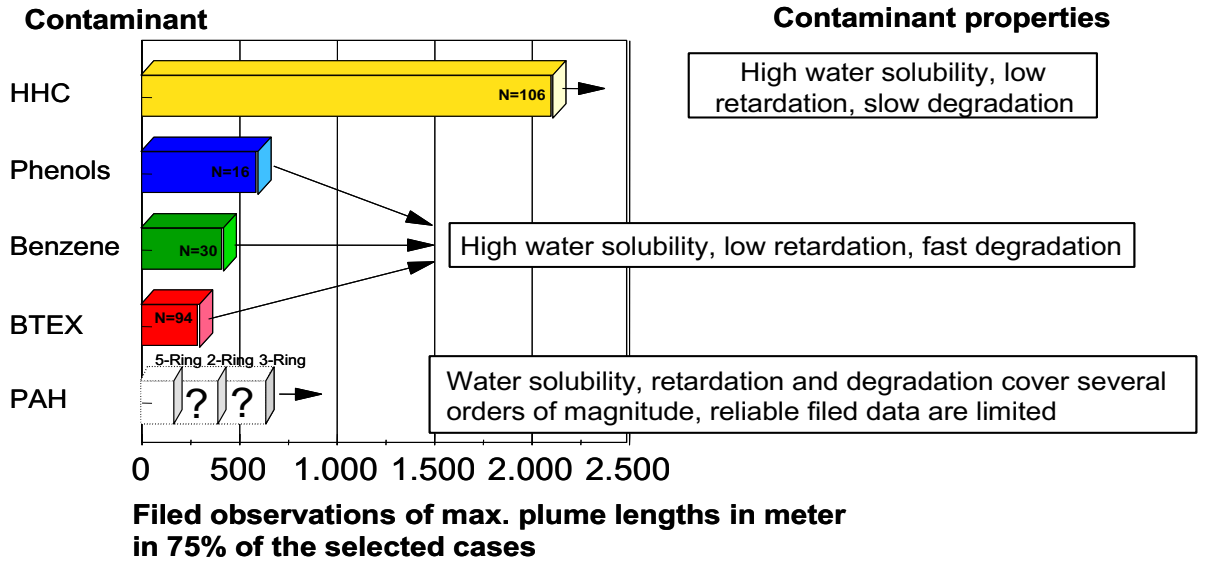

Fig. 1.1: Plumes lengths collected from field studies (N: number of observations)

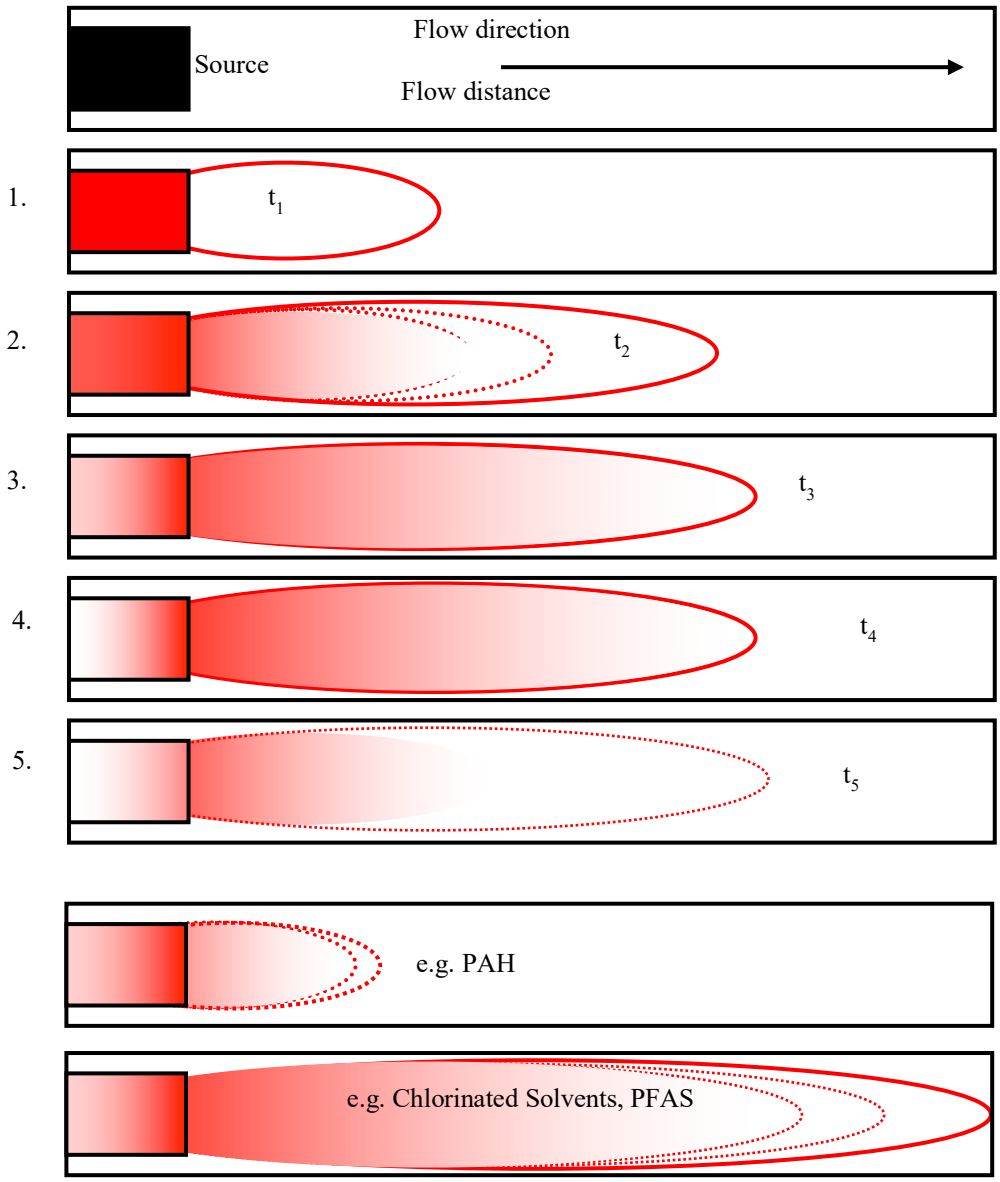

Fig. 1.2: Evolution of plumes during different stages (t_0-t_5); t_0: time zero (contaminant spill), dissolution of contaminants with groundwater flow starts in the source area; t_1: early period (maybe a few months), spreading of contaminants from the source, a plume forms; t_2: plume grows with time but if biodegradation starts growth slows down (dashed lines); t_3 (a few years): the plume reaches steady state conditions - contaminant emission rates (from the source) are balanced by degradation rates; t_4 (decades): source gets slowly depleted - contaminant emission stays still high and plume is at steady state; t_5 (aging of the source): contaminant emission from the source reduces, the plume shrinks; strongly sorbing compounds such as PAHs form only short plumes while stable and less sorbing compounds such as chlorinated solvents or PFAS grow rapidly to very long plumes.

2. LENGTH OF STEADY STATE PLUMES

2.1 REACTIVE TRANSPORT

If groundwater comes into contact with pollutant source zones it gets contaminated and downstream plumes will develop. If source zones are fairly stable, which is the case for contamination with NAPLs, plumes will continue to grow in length unless the contaminants are degraded. If the overall degradation rate is balanced by the contaminant emission rate from the source, a stable steady state plume establishes. Fig. 2.1 summarizes processes relevant for plume growth and degradation. Sorption causes retardation of plume spreading until steady state conditions are reached (storage terms such as sorption do not apply for steady state, $dC/dt = 0$). In many cases biodegradation depends on the supply of electron acceptors (e.g., O_2) across the margins of the plume, which react with a electron doner (e.g., hydrocarbons or ammonium) as shown in Fig. 2.1 (and Fig. 2.3). The end of the plume is reached after the supply of electron acceptor balances the mass of electron donor.

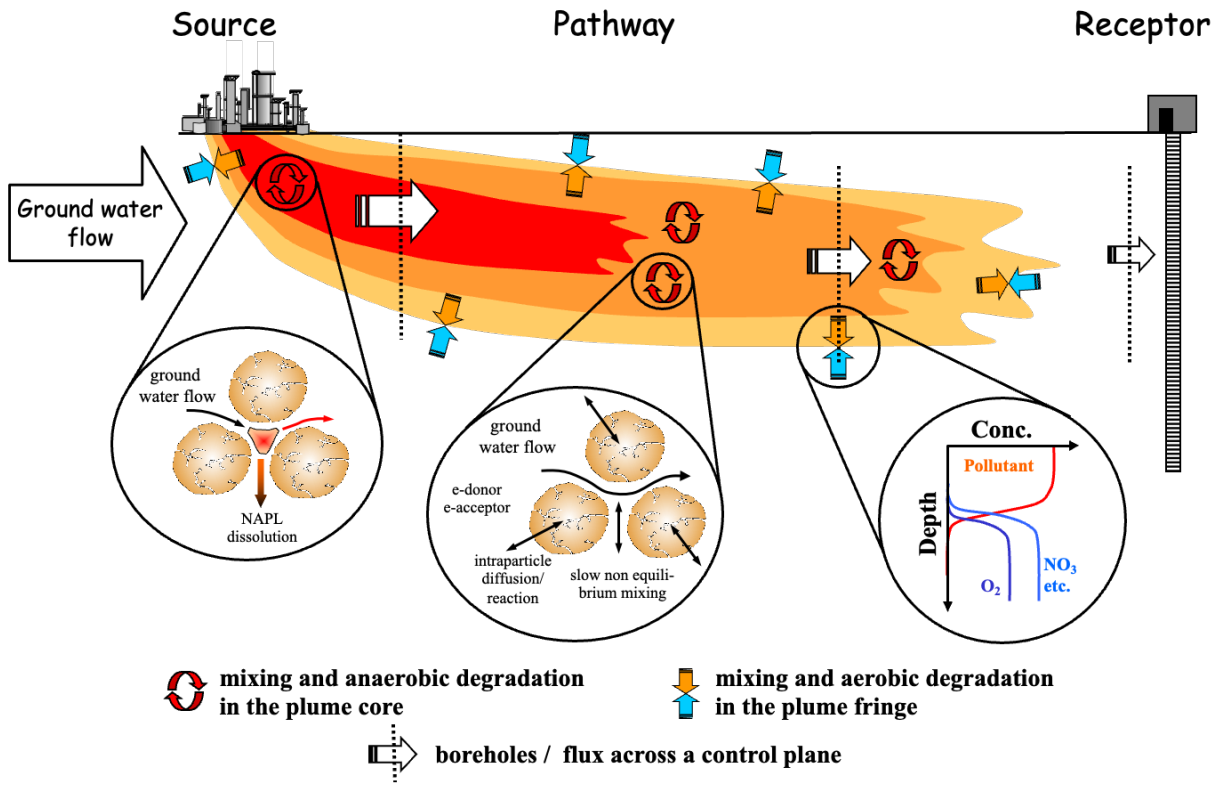

Fig. 2.1: Processes involved in plume growth

In such a scenario a reaction front moves into the plume as shown in Fig. 2.2 (Liu et al. 2010; Haberer et al., 2011, Haberer et al., 2015) and which is discussed in chap. 3 also for other simple "reaction - diffusion" problems. Theoretically the end of the plume is reached after the reaction front reached the bottom of the aquifer as depicted in Fig. 2.3. Liedl et al. (2005) derived a simple analytical solution to calculate the plume length for the scenario shown in Fig. 2.3:

$$L = \frac{4\,M^2\,v_a}{\pi^2\,D_t}\,\ln\left(\frac{4}{\pi}\,\frac{\gamma\,C_D + C_A}{C_A}\right) = \frac{4\,M^2}{\pi^2\,\alpha_t}\,\ln\left(\frac{4}{\pi}\left(\frac{\gamma\,C_D}{C_A} + 1\right)\right) \qquad (2.1)$$

M denotes the thickness of a plume which vertically extends over the entire aquifer. γ is a stoichiometric factor which accounts for how many mols of electron donor (C_D) are needed to consume one mol of electron acceptor (C_A); note, if mass-based concentrations are used, then γ will change. The right-hand term results from parametrizing the transverse dispersion coefficient (D_t) by the product of the transverse dispersivity and flow velocity ($D_t = \alpha_t\,v_a$). An empirical relationship was also developed for this scenario (Maier and Grathwohl, 2006):

$$L = 0.5\,\frac{M^2}{\alpha_t}\left(\frac{\gamma\,C_D}{C_A}\right)^{0.3} \qquad (2.2)$$

For similar scenarios see Ham et al. (2007), Cirpka et al. (2006) or Cirpka and Valocchi (2007). Eqs. 3.1 and 3.2 assume that the plume length depends on mixing of electron donor and acceptor and thus α_t, which in a porous medium is a function of pore scale processes (Hochstettler et al. 2013) but this may be also influenced by aquifer heterogeneity and structure (Werth et al., 2006; Ye et al., 2015, 2016). For more examples about dispersion dependent reactions in porous media see Haberer et al. (2014), Ye et al. (2014) or Muniruzzaman et al. (2014). An illustration of simplified conceptual models for plume lengths is given in the next chapter.

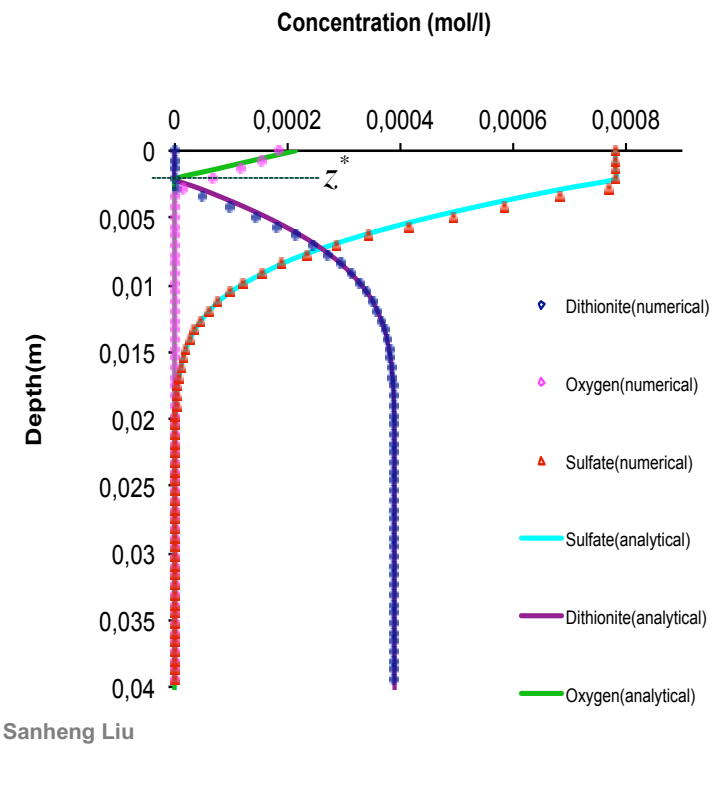

Vertical concentration profile of reactants (O_2, Na-dithionite) and product (sulfate). The water table is at 0.005 m. Reactants are at steady state whereas sulfate cannot escape to the gas phase and accumulates…

Analytical solution

$$z^* = 2\sqrt{D\frac{x}{v_a}}\;\mathrm{erfc}^{-1}\left(\frac{1}{\frac{C_{EA}}{\gamma C_{ED}}+1}\right)$$

for arguments ß between 0.25 and 1,

erfc^{-1}(ß) approaches 1 - ß =>

$$z^* \approx 2\sqrt{D\frac{x}{v_a}}\left(1-\frac{1}{\frac{C_{EA}}{\gamma C_{ED}}+1}\right)$$

$$= 2\sqrt{D\frac{x}{v_a}}\left(\frac{1}{\frac{\gamma C_{ED}}{C_{EA}}+1}\right)$$

Fig. 2.2: Movement of a O_2 reaction front into a plume (from the top); from Liu et al. 2012 (more exact approx. of erfc^{-1}(ß) is $(\mathbf{1}-ß)\sqrt{\boldsymbol{\pi/4}}$); for small arguments the approx. is $\sim\sqrt{-\mathbf{ln}(ß)}$

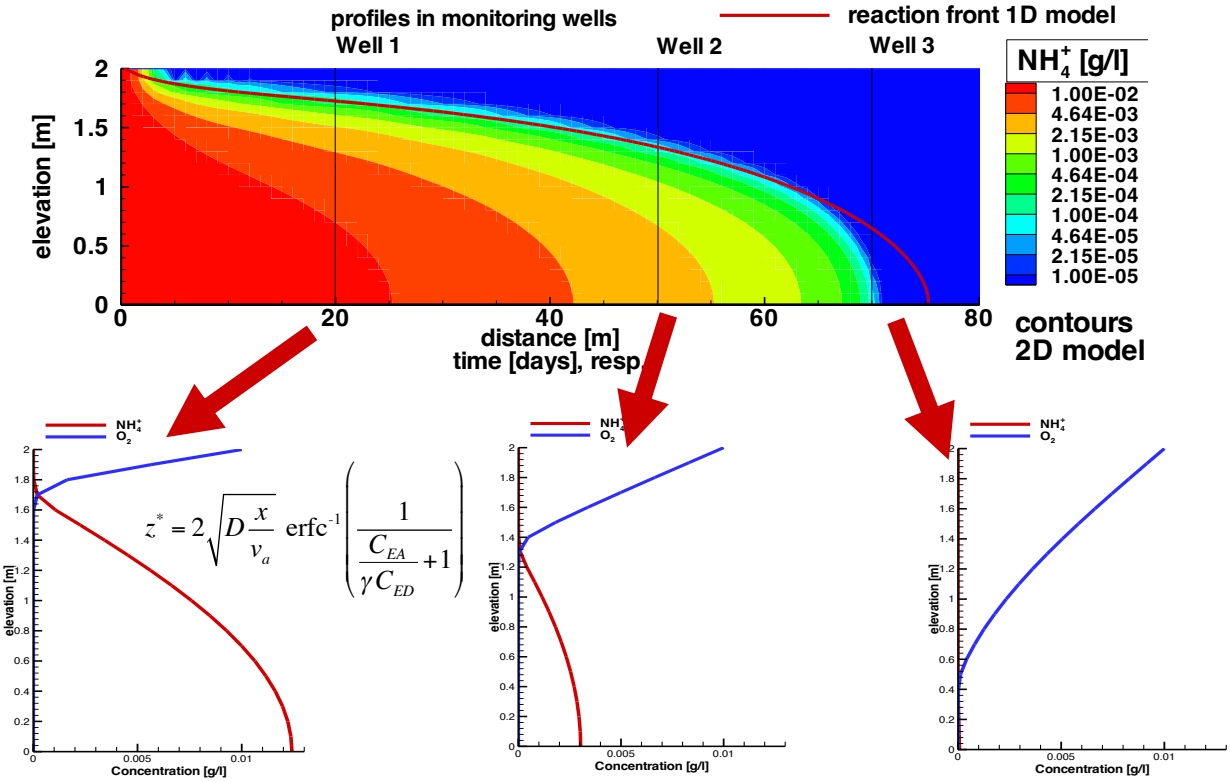

Fig. 2.3: Vertical profiles of electron donor (NH_4^+) and acceptor (O_2) concentrations in a steady state plume

Fig. 2.4 shows an example of the distribution of reactants and biomass for the case of an ammonium plume originating from a landfill which is a frequent scenario (waste filled sand and gravel pits); microbes preferentially settle where both electron donor and acceptor are available (Kappler et al., 2005). From such field investigations real world dispersivities may be calculated by using numerical reactive flow and transport models; some results are summarized in Table 2.1 which shows that in contrast to small scale laboratory investigations dispersivity at the field scale amounts often to several centimeters.

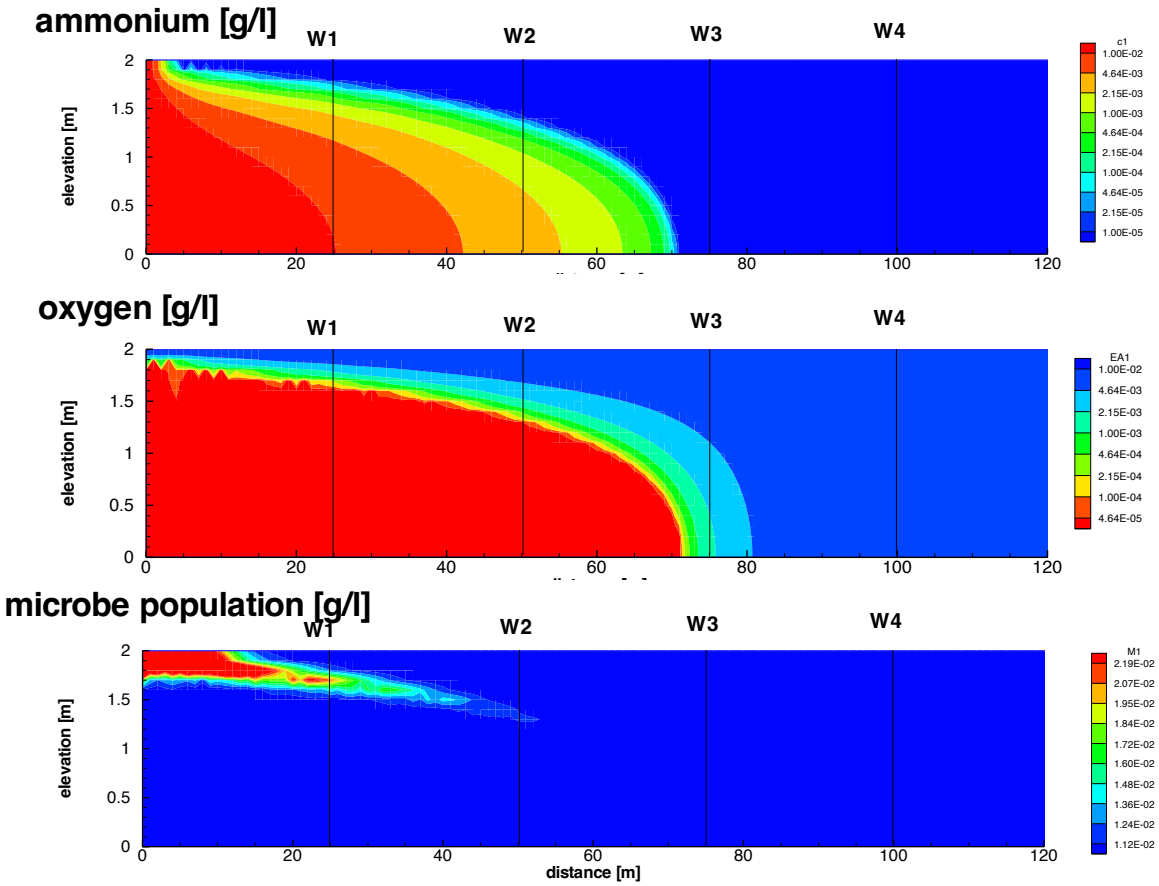

Fig. 2.4: Ammonium plume with O_2 and microbial biomass distribution

Tab. 2.1: Field scale dispersivities obtained from ammonium plumes reacting with O_2 at former landfill sites in quarternary sand and gravel deposits

Site velocity	NH_4^+ (mg/l)	M_{Cont} (m)	M_{Aqu} (m)	L_{PLUME} (m)	α_t (cm)	Model
Oster-hofen 2.7 m/d	15	4.5	4.5	580	**3.2**	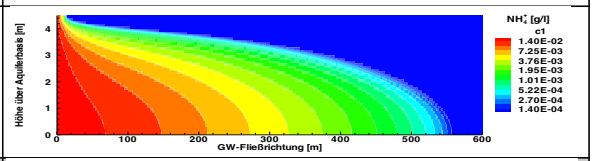
Röschen-wasser 2.65 m/d	1.5	0-3	12	400 - 140	**1 - 3**	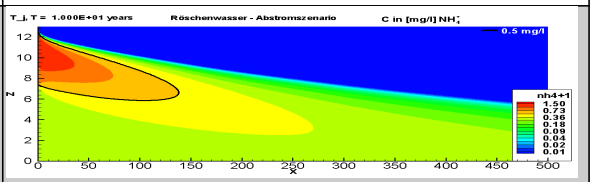
	1.0	3-5				
	0.3	5-12				
Seehof 1 m/d	5	0-3	14	5 500 - 1 700	**3 – 10**	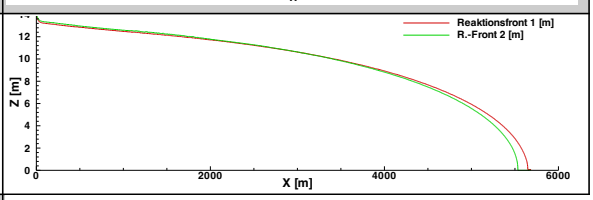
	17	3-14				
Cattun-lache 0.1 m/d	9	0-9	70	11 000	**10**	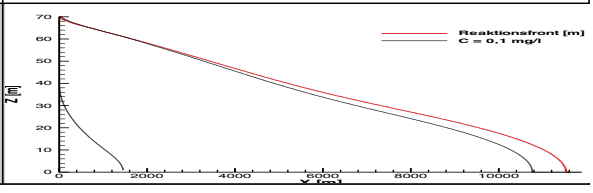
	5	9-30				
	0	30-70				

2.2 RELEVANCE OF DIFFERENT BOUNDARY CONDITIONS FOR PLUME LENGTH APPROXIMATIONS

Plume lengths depend much on boundary conditions and thus on the conceptual model used in reactive transport simulations. Here very simplified approaches based on boundary layers are described which help to understand the most important parameters. For example, if we take the scenario depicted in Fig. 2.3, the maximum plume length is achieved after the total mass of electron acceptor which has to diffuse into the plume domain in order to match the electron donor mass and to fill the pore space:

$$\gamma\, C_D\, n\, v_a\, M\, t = \frac{D_t\, n}{\delta}\, C_A\, L\, t \tag{2.3}$$

M denotes the thickness of a plume which vertically extends over the entire aquifer, v_a and n are groundwater flow velocity and porosity ($v_a\, n$ is the Darcy velocity) and C_D is the electron donor concentration in the source (γ is the stoichiometric coefficient. δ is the thickness of a mass transfer boundary layer for supply of the electron donor with a fixed concentration (C_A) at the groundwater table. Since the end of the plume (L) is reached after the reaction front reaches the bottom of the aquifer (see Fig. 2.3), the half thickness of the aquifer ($M/2$) may be used for estimating the unknown δ in a first approximation:

$$\gamma\, C_D\, n\, v_a\, M = \frac{D_t\, n}{M/2}\, C_A\, L \tag{2.4}$$

Using the classical parameterization for the dispersion coefficient ($D_t = \alpha_t\, v_a$) and re-arranging yields for the plume length L:

$$\begin{aligned} \gamma\, C_D\, v_a\, M &= \frac{\alpha_t\, v_a}{M/2}\, C_A\, L \\ \rightarrow \quad L &= \frac{M^2}{2\,\alpha_t}\,\frac{\gamma\, C_D}{C_A} \end{aligned} \tag{2.5}$$

Thus, using this approach results in plume lengths depending linearly on the stoichiometric term ($\frac{\gamma\, C_D}{C_A}$).

Similarly to this vertical cross section scenario, we may use a horizonal (flat) source, but now with infinite boundary conditions (e.g. C_A = constant at $y = \infty$) like the case illustrated in Box 2.1. The unknown δ in eq. 2.3 may now be replaced by the mean square displacement ($= (\pi/4\, D_t\, t)^{0.5} = (\pi/4\, \alpha_t\, x)^{0.5}$):

$$\begin{aligned} \gamma\, C_D\, n\, v_a\, M &= \frac{\alpha_t\, v_a\, n}{\sqrt{\pi/4\, \alpha_t\, L}}\, 2\, C_A\, L \\ \rightarrow \quad L &= \frac{\pi\, M^2}{16\, \alpha_t}\left(\frac{\gamma\, C_D}{C_A}\right)^2 \end{aligned} \tag{2.6}$$

This corresponds to the solution of Chu et al. (2005) and is similar to the solution of Ham et al. (2004) or Cirpka et al. (2006) for a point injection or a planar source of the electron donor ($L = \frac{M^2}{16\,\alpha_t}\, 4/\pi \left(\frac{\gamma\, C_D}{C_A} + 1\right)^2$). In all these solutions for the estimation of plume lengths the source term enters squared (M^2) and the length increases proportionally to $1/\alpha_t$. They differ, however, significantly concerning the sensitivity of the stochiometric term. While

in the Liedl et al. (2005) solution (vertical cross section, finite boundaries) the plume length grows with $\ln\left(\frac{4}{\pi}\left(\frac{\gamma\, C_D}{C_A}+1\right)\right)$, eq. 2.5 suggests a linear dependency, while eq. 2.6 and the conceptual model in Box 2.1 results in a square dependency (as in Ham et al., 2004). These simple considerations indicate that plume lengths depend very much on the boundary conditions chosen in the conceptual model especially if the stochiometric term is large ($\gamma\, C_D >> C_A$), which typically is the case; a comparison is shown in Fig. 2.5. As Chu et al. (2005) point out, the solution with the quadratic term $\left(\frac{\gamma\, C_D}{C_A}\right)^2$ results in unrealistic long plumes. Therefore, the selection of the appropriate boundary conditions is crucial in estimating plume lengths. Since most shallow aquifers have large lateral extensions compared to their thickness (like a "pancake") the Liedl et al. (2005) solution appears more generally applicable. For more complicated boundary geometries numerical solutions must be employed for accurate assessment of plume lengths.

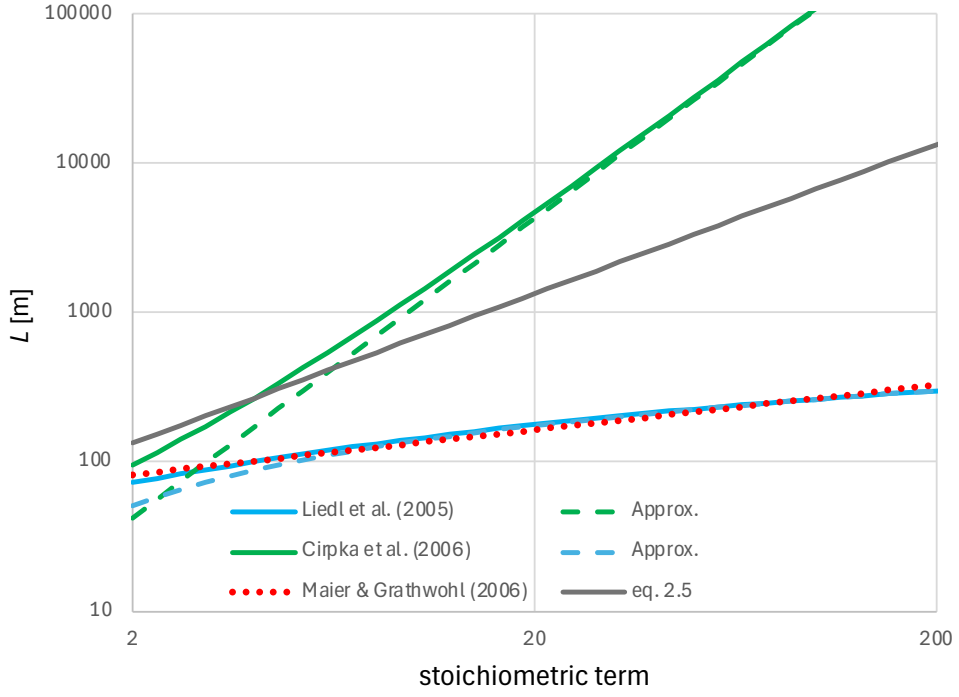

Fig. 2.5: Plume length (L) vs. stoichiometric term ($\gamma\, C_D/C_A + 1$); approx. for $\gamma\, C_D >> C_A$ ($= \gamma\, C_D/C_A$)

Box 2.1: A simplified boundary layer model for plume lengths

Plume lengths may be estimated by balancing the amount of electron acceptor (EA) needed to oxidize the total amount of electron donor (ED) in a plume. The total mass of electron donor released from a source area (A_{source}) after time t at flow velocity v_a is:

$$M_D = v_a n\, C_D A_{source}\, t$$

The mass of electron acceptor (EA) needed to oxidize M_D and to fill the pore space (initially void of EA) which has to transferred across the plume area through a boundary layer into the plume can be determined by a mass balance:

$$A_{source}\, v_a\, n\, \gamma\, C_D\, t = D_t\, n \frac{C_A}{\sqrt{D_t\, t}} A_{plume}\, t$$

D_t is the transverse dispersion coefficient, multiplied by the porosity (n) and divided by a boundary layer thickness ($\approx \sqrt{D_T\, t}$) yields a mass transfer coefficient. γ is a stoichiometric factor (e.g. how many moles of EA are needed to oxidize the ED). Source and plume areas for a square source with height M and a plume of length L are simply M^2 and 4 M L:

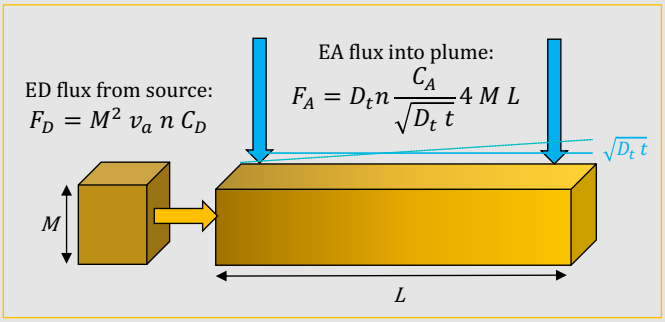

D_t may be parametrized as $\alpha_t\, v_a$ and if the contact time is given by L/v_a then this leads to:

$$M^2\, v_a\, \gamma\, C_D\, t = \alpha_t\, v_a \frac{C_A}{\sqrt{\alpha_t\, v_a\, L/v_a}} 4\, L\, M\, t$$

$$M\, \gamma\, C_D = \alpha_t \frac{C_A}{\sqrt{\alpha_t\, L}} 4\, L = 4\sqrt{\alpha_t\, L}\, C_A$$

This can be solved for L:

$$L = \frac{M^2}{16\, \alpha_t} \left(\frac{\gamma\, C_D}{C_A}\right)^2$$

The same solution is obtained for a radial source and a cylindrical plume (A_{source} = $(M/2)^2\, \pi$; A_{plume} = 2 π $(M/2)$ L)); for a cone shaped plume (A_{plume} = π $(M/2)$ L)) the geometric factor in the denominator becomes 4 instead of 16 (as in eq. 2.6). This comes close to the solution provided for plane or point sources with infinite boundaries (e.g., Ham et al., 2004, Chu et al., 2005, Cirpka et al., 2006; Cirpka and Valocchi, 2007):

$$L = \frac{M^2}{16\, \alpha_t \left(\text{inverf}\left(\frac{C_A}{\gamma C_D + C_A}\right)\right)^2} \approx \frac{M^2}{16\, \alpha_t} \frac{4}{\pi} \left(\frac{\gamma C_D + C_A}{C_A}\right)^2 \approx \frac{M^2}{16\, \alpha_t} \left(\frac{\gamma C_D}{C_A} + 1\right)^2 \approx \frac{M^2}{16\, \alpha_t} \left(\frac{\gamma C_D}{C_A}\right)^2$$

The first term denotes the Cirpka et al. (2006) solution, the first approximation is for small agruments (ß < 0.5) in inverf (inverf (ß))^2 ≈ 1/(4/π 1/ß^2) ≈ ß^2) and the second for $\gamma\, C_D / C_A >> 1$.

This of course is only valid in an infinite and homogeneous porous medium which does not likely correspond to real plumes and for such cases numerical solution likely are needed.

2.3 REACTIVE PLUMES FROM THE DISSOLUTION OF NAPL-POOLS

Similar to the progress of an oxidation front shown in Fig. 2.2 the thickness of a reactive plume may be estimated for transport of the electron donor (e.g. fuel hydrocarbon) across the capillary fringe into an aerobic aquifer (following Liu et al., 2010, but ED and EA are switched) or the dissolution of a DNAPL pool at the bottom of an aquifer (e.g. coal tar with electron donors):

$$M = \sqrt{\alpha_t \, L_{source}} \, \sqrt{\pi/4} \left(\frac{1}{\frac{C_A}{\gamma \, C_D} + 1} \right) \approx \sqrt{\alpha_t \, L_{source}} \tag{2.8}$$

The approximation is for a strong electron donor (high $\gamma \, C_D$ – so not much biodegradation in the source), then its spreading is not affected by the degradation (it behaves like a tracer). For a strong EA (or weak ED) only thin plumes develop downgradient of the source. Inserting the first part into the approximate plume length equation for infinite boundary conditions leads to:

$$L = \frac{M^2}{16 \, \alpha_t} \left(\frac{\gamma C_D}{C_A} + 1 \right)^2 = \frac{\alpha_t \, L_{source} \left(\frac{1}{\frac{C_A}{\gamma \, C_D} + 1} \right)^2}{16 \, \alpha_t} \left(\frac{\gamma \, C_D}{C_A} + 1 \right)^2 = \frac{L_{source}}{16} \left(\frac{\gamma \, C_D}{C_A} \right)^2 \tag{2.9}$$

Since the transverse dispersivity determines both, the source strength and the plume length it cancels out. This solution neglects a potential supply of electron acceptor (e.g. O_2) across the capillary fringe downstream of the source, which would shorten the plume considerably. For the dissolution of DNPL pools downgradient diffusion of the electron donor in low permeability layers is neglected. The scenario works also for floating LNAPL at the groundwater table.

3. "REACTION - DIFFUSION" EXAMPLES

3.1 VOLATILIZATION

Many NAPL constituents (e.g., in in fuels like "gasoline") are volatile and may evaporate from subsurface spills to the atmosphere. Fig. 3.1 illustrates volatilization from residual phase and Fig. 3.2 from NAPL layers floating on the groundwater table additionally affected by biodegradation. The advancement of a volatilization front as shown in Fig. 3.1 may be easily calculated by setting the mass lost to the atmosphere equal to the mass removed from the subsurface as shown in eq. 3.1. As the example shows, this is fairly slow and therefore ventilation systems typically are employed to remove the contamination in such cases. So-called "soil vapor extraction systems" are among the most powerful and efficient remediation technologies for removal of organic compounds from the unsaturated zone.

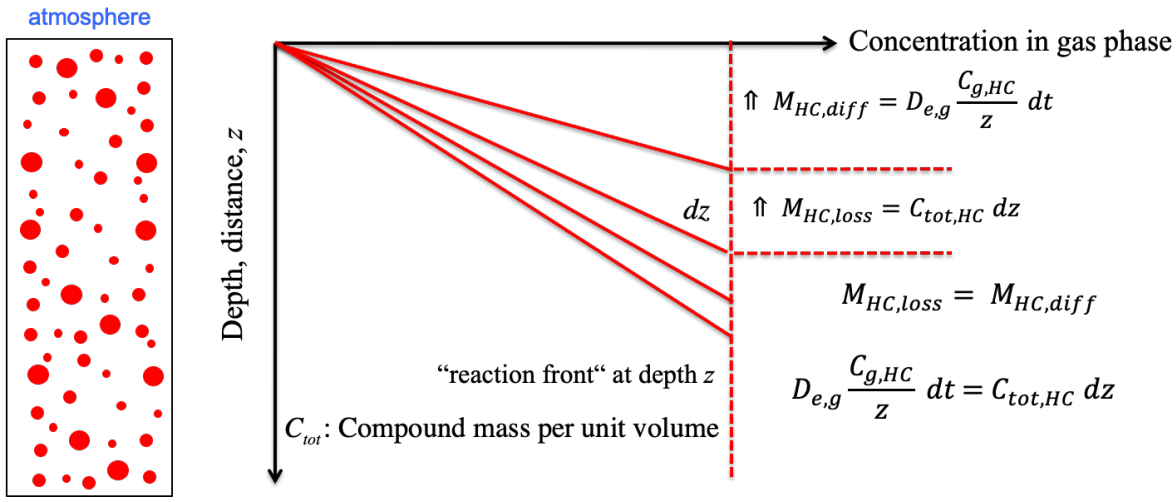

Fig. 3.1: Volatilization of residual hydrocarbons (red blobs) from the unsaturated soil zone and the progress of the volatilization front; $M_{HC,diff}$, $M_{HC,diff}$: mass diffused to the atmosphere and mass lost from the porous medium, $D_{e,g}$, $C_{g,HC}$: effective diffusion coefficient and saturation concentration of hydrocarbon in gas phase; similar approaches may be used to calculate e.g., the advance of a weathering (oxidation) front (see Fig. 3.3).

The depth of the volatilization front may be easily derived based on mass balance considerations (see also Fig. 3.1):

$$\int_0^t D_{e,g} C_{g,HC} dt = \int_0^z C_{tot,HC}\, z\, dz$$

$$D_{e,g} C_{g,HC}\, t = \frac{1}{2} C_{tot,HC}\, z^2 \qquad (3.1)$$

$$z = \sqrt{2\, D_{e,g} \frac{C_{g,HC}}{C_{tot,HC}}\, t} = \sqrt{\frac{2\, D_{e,g}}{n_g\, R_d}\, t} = \sqrt{\frac{2\, D_{p,g}}{R_d}\, t}$$

The product $n_g\, R_d$ is the capacity factor (α); $D_{e,g}/\alpha$ is a apparent diffusion coefficient and $D_{p,g}$ is a pore diffusion coefficient in gas phase. The retardation factor (R_d) in that case is (no sorption to soil solids considered):

$$R_d = \frac{total\ concentration}{mobile\ concentration} = \frac{C_{tot,HC}}{C_{g,HC}}$$
$$= \frac{C_{g,sat}\, n_g + \frac{C_{g,sat}\, n_w}{H} + n\, S^o_{NAPL}\rho_{NAPL}}{C_{g,sat}\, n_g} \qquad (3.2)$$
$$= 1 + \frac{n_w}{H\, n_g} + \frac{nS^o_{NAPL}\rho_{NAPL}}{C_{g,sat}\, n_g} \approx \frac{n\, S^\circ_{Napl}\, \rho_{Napl}}{C_{g,sat}}$$

For compound mixtures typically encountered in fuels, Raoult's law has to be employed, but since the fraction of a constituent in total mass also has to be considered in calculating the concentration in gas phase it drops out and $C_{g,sat}$ refers to the compound of interest in its pure state. The deeper the volatilization front progresses the lower the diffusion rates become and therefore removal by groundwater recharge may come into play. Fig. 3.2 compares both processes for a hypothetical case and shows that initially diffusion dominates but sooner or later seepage water advection takes over because the former progresses with the square root of time while the later advances linear with time (for retardation of the seepage water dissolution front see Box. 1.2). It should be noted that this feature generally applies: i.e., the movement of diffusion - reaction fronts dominates at early times or short distances and then advection takes over.

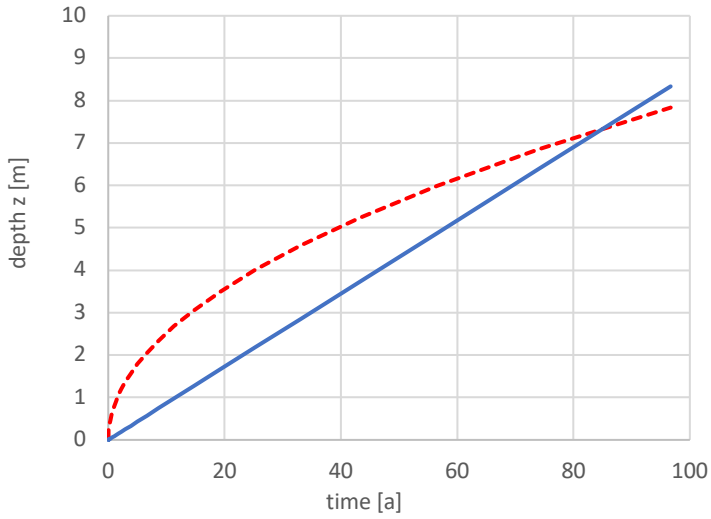

Fig. 3.2: Progress of a volatilization front in the unsaturated soil zone (dashed red) compared to dissolution by seepage water – at a certain point in time and space advection takes over (C_{sat} = 500 g m^{-3}, H = 0.2, D_g = 6 x 10^{-6} m^2 s^{-1}, n = 0.4, n_w (θ) = 0.14, n_g = 0.24, $\boldsymbol{S^o_{NAPL}}$= 5%, ρ_{NAPL} = 0.85 kg l^{-1} , recharge = 0.6 m a^{-1}, $R_{d,gas\ diffusion}$ = 146, $R_{d,recharge}$ = 44)

The scenario described above is quite hypothetical and could apply to smear zones with residual NAPL in the capillary fringe. More frequent are LNAPLs floating on the ground-water table. Since many LNAPL constituents (typical non-halogenated hydrocarbons in fuels) are easily aerobically biodegraded, the concentration gradients for volatilization may be steepened. Fig. 3.3 illustrates that for a fuel layer floating on the groundwater table ("pool"). The depth of the reaction zone (z) can be easily calculated setting the flux of the electron donor (hydrocarbon) equal to the flux of the electron donor (oxygen). This scenario is based on an instantaneous reaction (fast biodegradation) which is frequently observed and may be evaluated based on the Damköhler number which is the ratio of the reaction rate to the mass transfer rate. For Damköhler numbers larger than 10 mass transfer is limiting.

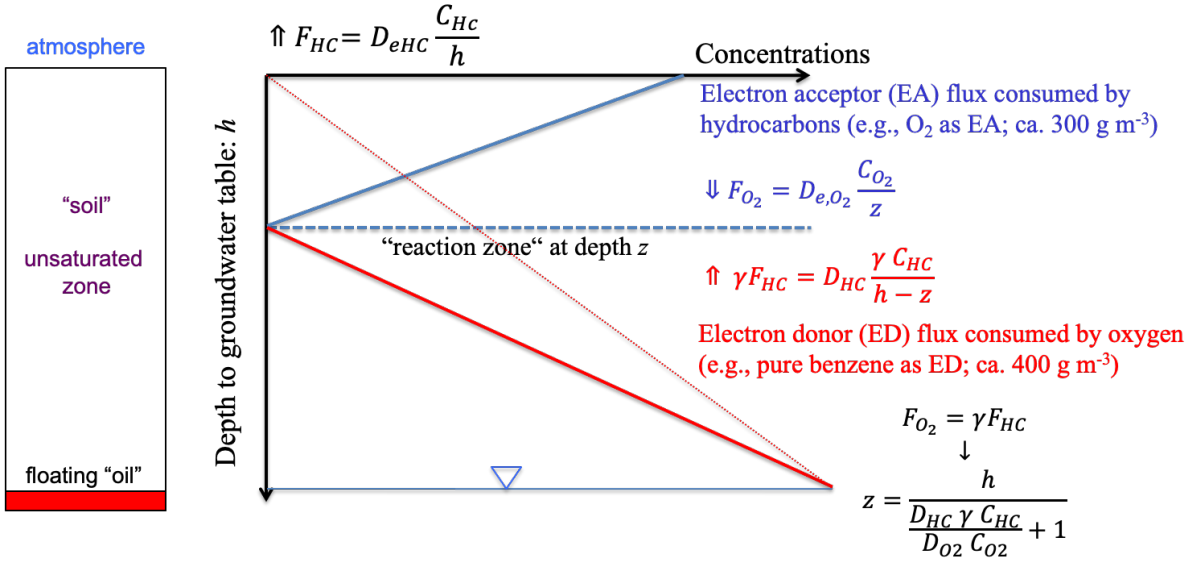

Fig. 3.3: Volatilization of residual hydrocarbons from a floating pool (red) enhanced by biodegradation in the unsaturated soil zone; F_{O2}, F_{HC}: fluxes of electron donors and acceptors; $D_{e,O2}$, D_{HC}: effective diffusion coefficient of oxygen and hydrocarbons in gas phase.

Box 3.1: Example for "reactive" volatilization

The scenario shown in Fig. 3.3 may be illustrated by the volatilization of benzene (or a similar compound). The "oxidation" stoichiometry in this case is: $C_6H_6 + 7.5\ O_2 = 6\ CO_2 + 3\ H_2O$; thus 7.5 moles of O_2 are needed for consumption of 1 mole of C_6H_6. Therefore, the flux of O_2 has to equal 7.5 times the flux of C_6H_6 ($F_{acceptor} = \gamma\ F_{donor}$). γ is the stoichiometric ratio (here 7.5 ➔ number of moles of O_2 consumed per mole C_6H_6). The depth (z) of the reaction zone relative to the distance to the groundwater table (h) is:

$$z = \frac{h}{\frac{D_{HC}\,\gamma\, C_{HC}}{D_{O_2}\, C_{O_2}} + 1}$$

D_{HC}, D_{O2} and C_{HC}, C_{O2} are the effective diffusion coefficients in the unsaturated soil zone and the concentrations of electron donor and acceptor at the boundaries; since this is based on the ratios of fluxes, only ratios of diffusion coefficients and concentrations are relevant. Examples for electron donor and acceptor concentrations are:

$$C_{benzene,air} = 400 \frac{\text{g}}{\text{m3}} \approx 5 \frac{\text{mol}}{\text{m3}}$$

$$C_{O2,air} = 0.21 \frac{\text{vol}}{\text{vol}} \approx 210 \frac{\text{liters}}{\text{m3}} = 9.4 \frac{\text{mol}}{\text{m3}}$$

(1 mol O_2 = 22.4 liters)

The depth of the reaction front is:

$$z = \frac{h}{\frac{D_{HC}\,\gamma\, C_{HC}}{D_{O_2}\, C_{O_2}} + 1} = \frac{h}{0.4 \cdot 7.5 \frac{5}{9.4} + 1} = \frac{h}{2.6}$$ ➔ 3.85 m (instead of 10 m)

Thus, the volatilization rate of the benzene is accelerated by more than twice by biodegradation.

4. LITERATURE

Chu, M., P. K. Kitanidis, and P. L. McCarty (2005), Modeling microbial reactions at the plume fringe subject to transverse mixing in porous media: When can the rates of microbial reaction be assumed to be instantaneous? Water Resour. Res., 41, doi:10.1029/2004WR003495.

Cirpka, O.A., Olsson, Ă., Ju, Q., Rahman, A., Grathwohl, P. 2006. Determination of transverse dispersion coefficients from reactive plumes lengths. Ground Water, 44, 212-221

Cirpka, O.A., Valocchi, A.J., 2007: Two-dimensional concentration distribution for mixing-controlled bioreactive transport in steady state. Adv. Water Resour. 30, 1668–1679

Haberer, C. M., Rolle, M., Cirpka, O. A., Grathwohl, P. 2014. Impact of Heterogeneity on Oxygen Transfer in a Fluctuating Capillary Fringe. Groundwater 53, 57-70, 2015, doi: 10.1111/gwat.12149

Haberer, C.M., Muniruzzaman, Md., Grathwohl, P., Rolle, M. 2015. Diffusive-dispersive and reactive fronts in porous media: Iron(II) oxidation at the unsaturated-saturated interface. Vadose Zone Journal, doi:10.2136/vzj2014.07.0091

Haberer, C.M., Rolle, M., Liu, S., Grathwohl, P. 2011. A high-resolution non-invasive approach to quantify oxygen transport across the capillary fringe and in the underlying groundwater. J. Cont. Hydrol. 122, 26-39, DOI: 10.1016/j.jconhyd.2010.10.00

Ham P.A.S., Schotting, R.J., Prommer, H., Davis, G.B. 2004. Effects of hydrodynamic dispersion on plume lengths for instantaneous bimolecular reactions. Adv. Water Resour., 27, 803–813

Ham P.A.S., Prommer, H., Olsson, A.H. Schotting, R.J., Grathwohl, P. 2007. Predictive modelling of dispersion controlled reactive plumes at the laboratory scale. J. Cont. Hydrol. 93, 304–315

Hochstetler, D.L., Rolle, M., Chiogna, G., Haberer, C.M., Grathwohl, P., Kitanidis, P.K. 2013. Effects of compound-specific transverse mixing on steady-state reactive plumes: Insights from pore-scale simulations and Darcy-scale experiments. Advances in Water Resources 54, 1–10

Kappler, A., Emerson, D., Edwards, K., Amend, J.P., Gralnick, J.A., Grathwohl, P., Hoehler, T., Straub, K. 2005. Microbial activity in biogeochemical gradients - new aspects of research. Geobiol., 3, 229-233

Lebedeva, M.I., Fletcher, R.C., Balashov, V.N., Brantley, S.L. 2007. A reactive diffusion model describing transformation of bedrock to saprolite. Chemical Geology, 244, 624–645

Liedl, R., Valocchi, A.J., Dietrich, P., Grathwohl, P. (2005): The finiteness of steady-state plumes. Water Resources Research, 41, 1-8, doi:10.1029/2005WR004000

Liu, S., Liedl, R., Grathwohl, P. 2010. Simple analytical solutions for oxygen transfer across the capillary fringe into anaerobic groundwater. Water Resour. Res., 46, doi:10.1029/2009WR008434

Maier, U., Grathwohl, P. 2006. Numerical experiments and field results on the size of steady state plumes. J. Cont. Hydrol., 85, 33-52

Maier, U., Rügner, H., Grathwohl, P. 2007. Gradients Controlling Natural Attenuation of Ammonium. Applied Geochemistry, 22, 2606–2617

Muniruzzaman, M., Haberer, C.M., Grathwohl, P., Rolle, M. 2014. Multicomponent ionic dispersion during transport of electrolytes in heterogeneous porous media: Experiments and model-based interpretation. Geochimica et Cosmochimica Acta, 141, 656 - 669

Werth, C. J., Cirpka, O. A., Grathwohl, P. 2006. Enhanced mixing and reaction through flow focusing in heterogeneous porous media, Water Resour. Res., 42, W12414, doi:10.1029/2005WR004511

Ye, Y., Chiogna, G., Cirpka, O., Grathwohl, P., Rolle, M. 2015. Experimental evidence of helical flow in porous media. Physical Review Letters, 115, 194502

Ye, Y., Chiogna, G., Cirpka, O., Grathwohl, P., Rolle, M. 2015. Enhancement of Plume Dilution in Two- and Three-Dimensional Porous Media by Flow Focusing in High-Permeability Inclusions. Water Resources Research, 51, 5582-5602

Ye, Y., Chiogna, G., Cirpka, O., Grathwohl, P., Rolle, M. 2016. Experimental investigation of transverse mixing in porous media under helical flow conditions. Phys. Rev. E 94, 013113, doi:10.1103/PhysRevE.94.013113

Ye, Y., Chiogna, G., Cirpka, O.A., Grathwohl, P., Rolle, M. 2014. Experimental investigation of compound-specific dilution of solute plumes in saturated porous media: 2-D vs. 3-D flow-through systems. Journal of Contaminant Hydrology, 172, 33-47 DOI: 10.1016/j.jconhyd.2014.11.002